

000 001 002 003 004 005 UNLEASHING THE POTENTIAL OF CONVNETS FOR 006 QUERY-BASED DETECTION AND SEGMENTATION 007 008 009

010 **Anonymous authors**
 011 Paper under double-blind review
 012
 013
 014
 015
 016
 017
 018
 019
 020
 021
 022
 023
 024
 025
 026
 027
 028
 029

030 ABSTRACT 031

032 Transformer and its variants have shown great potential for various vision tasks
 033 in recent years, including image classification, object detection and segmentation.
 034 Meanwhile, recent studies also reveal that with proper architecture design,
 035 convolution networks (ConvNets) also achieve competitive performance with trans-
 036 formers, *e.g.*, ConvNeXt. However, no prior methods have explored to utilize pure
 037 convolution to build a Transformer-style Decoder module, which is essential for
 038 Encoder-Decoder architecture like Detection Transformer (DETR). To this end, in
 039 this paper we explore whether we could build query-based detection and segmenta-
 040 tion framework with ConvNets instead of sophisticated transformer architecture.
 041 We propose a novel mechanism dubbed InterConv to perform interaction between
 042 object queries and image features via convolutional layers. Equipped with the
 043 proposed InterConv, we build Detection ConvNet (DECO), which is composed of
 044 a backbone and convolutional encoder-decoder architecture. We compare the pro-
 045 posed DECO against prior detectors on the challenging COCO benchmark. Despite
 046 its simplicity, our DECO achieves competitive performance in terms of detection
 047 accuracy and running speed. Specifically, with the ResNet-18 and ResNet-50 back-
 048 bone, our DECO achieves 40.5% and 47.8% AP with 66 and 34 FPS, respectively.
 049 The proposed method is also evaluated on the segment anything task, demon-
 050 strating similar performance and higher efficiency. We hope the proposed method brings
 051 another perspective for designing architectures for vision tasks.
 052
 053

1 INTRODUCTION

034 Object detection and segmentation are among the most foundational computer vision tasks and
 035 are essential for many real-world applications (Ren et al., 2015; Redmon & Farhadi, 2017; 2018;
 036 Bochkovskiy et al., 2020). The object detection pipeline has been developed rapidly, especially
 037 in the era of deep learning. Faster R-CNN (Ren et al., 2015) is one of the most typical two-stage
 038 object detectors, which utilizes a coarse-to-fine framework for bounding box prediction. Meanwhile,
 039 one-stage detectors like SSD (Liu et al., 2016), YOLO series (Redmon & Farhadi, 2017; 2018;
 040 Bochkovskiy et al., 2020) or FCOS (Tian et al., 2019) *etc.* simplify the detection pipeline by directly
 041 predicting the objects of interest from the image features. Most of the above object detectors are
 042 built upon convolutional neural networks (CNNs or ConvNets) and typically the Non-maximum
 043 Suppression (NMS) strategy is utilized for post-processing to remove duplicated detection results.
 044

045 The advancement of deep neural architectures have been benefiting the task of object detection. For
 046 example, more powerful architectures usually bring considerably significant improvement for the
 047 detection performance (Li et al., 2018; Liu et al., 2020; Gao et al., 2019; Guo et al., 2020). Recently
 048 the emergence of vision transformer and its variants (Dosovitskiy et al., 2021; Liu et al., 2021;
 049 Touvron et al., 2021; Wang et al., 2021b) have shown prominent performances on image classification
 050 tasks and have built a solid foundation for the object detection field. Carion *et al.* (Carion et al.,
 051 2020) proposes the Detection Transformer (DETR) that refactors the object detection pipeline as a
 052 set prediction problem and directly obtains a fixed set of objects via a transformer encoder-decoder
 053 architecture. This design enables DETR to get rid of the complicated NMS post-processing module
 054 and results in a query-based end-to-end object detection pipeline. There are quite a lot of variants to
 055 improve DETR via different aspects, *e.g.*, training convergence (Meng et al., 2021; Gao et al., 2021),
 056 multi-scale features and deformable attention (Zhu et al., 2021) or better query strategy (Li et al.,
 057 2022; Liu et al., 2022a; Wang et al., 2022; Zhang et al., 2022), *etc.*

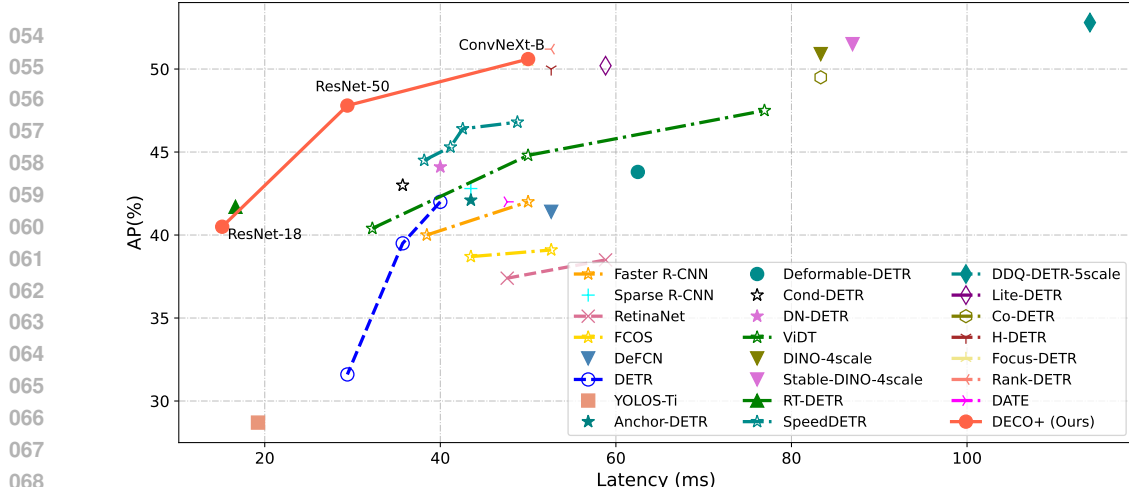


Figure 1: Comparisons of our proposed Detection ConvNets (DECO) and recent detectors on COCO *val* set. The latency is measured on a NVIDIA V100 GPU.

Despite the strong performance of transformer, it does introduce more challenges for AI chips (Tu et al., 2022). More specifically, attention layers introduce dynamic memory access whose weights and inputs are both generated during runtime. On contrast, convolutional layers have static memory access since weights do not change during inference. Therefore, it is still common that certain operators like attention module is not well supported in some AI chips, which is a big challenge in industry.

Meanwhile, some recent work rethinks the strong performance and reveal that the pure ConvNets could also achieve competitive performance via proper architecture design (Liu et al., 2022b; Yu et al., 2022). For example, ConvNeXt (Liu et al., 2022b) competes favorably with vision transformers like Swin Transformer (Liu et al., 2021) in terms of accuracy and computational cost. However, these methods mainly focus on Encoder part of transformer, in which self-attention is utilized and could be replaced by convolution with careful design. These motivate us to explore one important question in this paper: *could we obtain an architecture via pure ConvNets but still enjoys the excellent properties similar to attention?*

In this paper, we propose a novel mechanism dubbed **InterConv** to perform interaction between object queries and image features via convolutional layers. It works similar with attention mechanism but simply built with pure convolution. We abstract the general architecture of decoder and divide it into two components, *i.e.*, Self-Interaction Module (SIM) and Cross-Interaction Module (CIM). In transformer-based models, the SIM and CIM are implemented with multi-head self-attention and cross-attention mechanism, while they are obtained with our proposed InterConv in our method. The Self-InterConv is stacked with simple depthwise and 1×1 convolutions. We further carefully design a novel Cross-InterConv mechanism to perform interaction between object queries and image features via convolutional layers as well as simple upsampling and pooling operations.

Equipped with the proposed InterConv, we develop **Detection ConvNet (DECO)**, which is a simple yet effective query-based end-to-end object detection framework. Our DECO model enjoys the similar favorable attributes as DETR. For example, using the mechanism of object query, our DECO directly obtains a fixed set of object predictions and also discards the NMS procedure. Moreover, it is stacked with only standard convolutional layers and does not rely on any sophisticated attention modules. To achieve this goal, we first carefully revisit the design of DETR and propose the DECO encoder and decoder architectures as shown in Fig. 3. The DECO encoder is built upon ConNeXt blocks and no positional encodings are necessary since ConvNets are variant to input permutation.

We evaluate the proposed DECO on the challenging object detection benchmark, *i.e.*, COCO (Lin et al., 2014). Experimental results demonstrate that our DECO achieves competitive performance in terms of detection accuracy and running speed, as shown in Fig. 1. Specifically, with the ResNet-18 and ResNet-50 backbone (He et al., 2016), our DECO achieves 40.5% and 47.8% AP with 66 and 34 FPS, respectively and outperforms the DETR model. Extensive ablation studies are also conducted to provide more discussions and insights about the design choices. We also apply the proposed method into the popular segment anything task. Our DECO-TinySAM obtains quite similar performance and

108 higher efficiency on mobile phone with the TinySAM baseline, demonstrating the effectiveness of
 109 our proposed method.
 110

111 The main contributions can be summarized as follows: (1) In this paper, we propose a novel
 112 mechanism dubbed **InterConv** to perform interaction between object queries and image features via
 113 convolutional layers. (2) Equipped with the proposed InterConv, we propose a novel query-based end-
 114 to-end object detection framework built with standard convolutions, *i.e.*, Detection ConvNet (DECO),
 115 which is simple yet effective. (3) The proposed method also demonstrates excellent performance on
 segment anything task.
 116

117

118 2 RELATED WORK 119

120

121 **Object Detection.** Object detection is one of the most foundational computer vision task and has
 122 attracted large amount of research interest from the computer vision community. The object detection
 123 pipeline has been developed rapidly, especially in the era of deep learning. Faster R-CNN (Ren et al.,
 124 2015) is one of the most typical two-stage object detectors, which first generates region proposal and
 125 extracts regional features for final bounding box prediction. Two-stage detection pipeline has been
 126 improve from various aspects (Pang et al., 2019; Cai & Vasconcelos, 2018). Meanwhile, one-stage
 127 detectors like SSD (Liu et al., 2016), YOLO series (Redmon et al., 2016; Redmon & Farhadi, 2017;
 128 2018; Bochkovskiy et al., 2020), CenterNet (Zhou et al., 2019; Duan et al., 2019) or FCOS (Tian
 129 et al., 2019) simplify the detection pipeline by directly predicting the objects of interest from the
 130 image features (Li et al., 2019; Lu et al., 2019; Zhu et al., 2019; Kong et al., 2019; Zhu et al., 2020;
 Law et al., 2020; Zhang et al., 2020).

131

132 **Transformer-based End-to-End Detectors.** The pioneering work DETR (Carion et al., 2020)
 133 utilizes a transformer encoder-decoder architecture and models the object detection as a set prediction
 134 problem. It directly predicts a fixed number of objects and get rid of the need for hand-designed
 135 non-maximum suppression (NMS) (Neubeck & Van Gool, 2006). More follow-up studies (Meng
 136 et al., 2021; Gao et al., 2021; Dai et al., 2021a; Wang et al., 2022) have made various optimizations
 137 and extensions based on the original DETR and achieve strong detection performance. For example,
 138 Deformable DETR (Zhu et al., 2021) only attends to a small set of key sampling points by introducing
 139 multi-scale deformable self/cross-attention to improve the detection accuracy as well as the training
 140 convergence. DAB-DETR (Liu et al., 2022a) improves DETR by using box coordinates as queries in
 141 decoder. DN-DETR and DINO (Li et al., 2022; Zhang et al., 2022) introduce several novel techniques,
 142 including query denoising, mixed query selection *etc.*, to achieve strong detection performance. RT-
 143 DETR (Lv et al., 2023) designs the first real-time end-to-end detector, in which an efficient multi-scale
 144 hybrid encoder and an IoU-aware query selection are proposed. One of the most important properties
 145 for DETR-based detectors is the query-based scheme for producing the final predictions, which
 146 streamlines the detection pipeline and make it an end-to-end detector.
 147

148

149 **ConvNet-based End-to-End Detectors.** Inspired by the success of transformer-based detector like
 150 DETR variants, several studies also attempt to remove the post-processing NMS by introducing
 151 one-to-one assignment strategy (Sun et al., 2021a; Wang et al., 2021a) and set prediction loss (Sun
 152 et al., 2021b). OneNet (Sun et al., 2021a) systematically explores the importance of classification cost
 153 in one-to-one matching and applies it on typical ConvNet-based detectors like RetinaNet (Lin et al.,
 154 2017) and FCOS (Tian et al., 2019). DeFCN (Wang et al., 2021a) introduces a new strategy of label
 155 assignment to enhance the matching cost. Sparse R-CNN (Sun et al., 2021b) integrates the fixed
 156 number of learnable anchor to a two-stage detection pipeline. However, it interacts query and RoI
 157 feature by the dynamic head which is a kind of learnable matrix multiplication.
 158

159

160 ConvNets have been demonstrated to have competitive performance on various tasks and are
 161 deployment-friendly in most hardware platforms (Liu et al., 2022b; Yu et al., 2022). Cheng *et*
 162 *al.* proposed SparseInst (Cheng et al., 2022), an efficient and fully convolutional framework for
 163 real-time instance segmentation. SparseInst utilizes a sparse set of instance activation maps to predict
 164 objects in end-to-end style, which could be viewed as an alternative for the query-based mechanism of
 165 DETR. In this paper we would like to design a DETR-like detection pipeline but built with standard
 166 convolutions, which could inherit both the advantages of ConvNets and the favorable properties of the
 167 DETR framework. Compared with SparseInst, our method follows the similar query-base mechanism
 168 of DETR, and also demonstrates good generalization capability like segment anything models.
 169

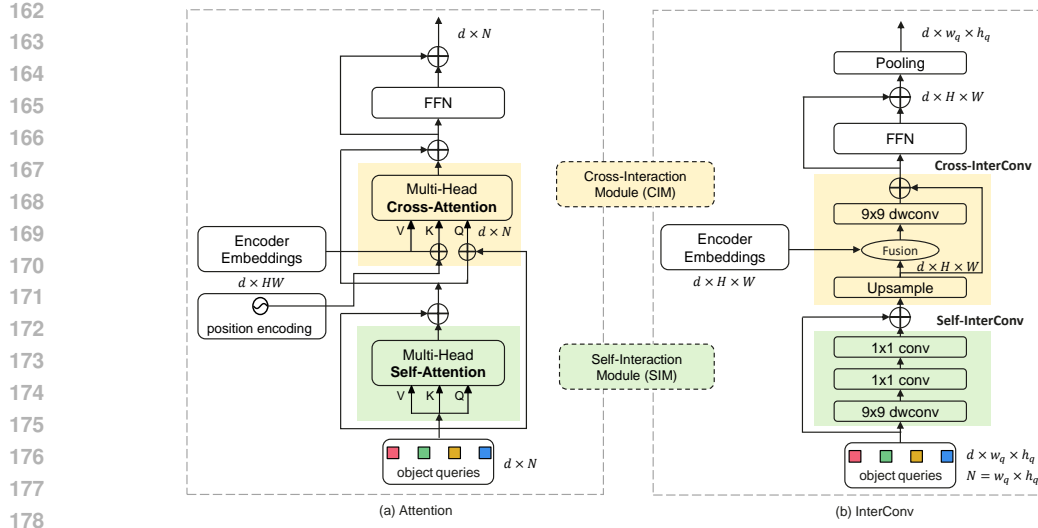


Figure 2: The attention-based decoder and our proposed InterConv. We abstract the general architecture of decoder and divide it into two components, *i.e.*, Self-Interaction Module (SIM) and Cross-Interaction Module (CIM). In DETR the SIM and CIM are implemented with multi-head self-attention and cross-attention mechanism, while in our proposed DECO, the SIM is stacked with simple depthwise and 1×1 convolutions. We further propose a novel CIM mechanism for our DECO to perform interaction between object queries and image features via convolutional layers as well as simple upsampling and pooling operations.

3 APPROACH

In this section, we first introduce the design of our proposed InterConv, which works similar with attention mechanism but simply built with pure convolution. We then provide details about utilizing InterConv to develop efficient models for detection and segmentation.

3.1 INTERCONV: BUILDING ATTENTION-LIKE MECHANISM WITH CONVOLUTION

Given a small set of object queries, the decoder in transformer-based models like DETR or SAM aims to reason the relations of the objects and the global image feature. As shown in Fig. 2 (a), each layer in transformer decoder is mainly composed of a self-interaction module (SIM) and a cross-interaction module (CIM). The self-interaction module (SIM) in original DETR is a multi-head self-attention layer and is responsible for interacting information between the object queries. The cross-interaction module (CIM) is the essential part for DETR decoder, which consists of cross-attention layer to perform interaction between the image embeddings from the output of encoder and the object queries. In this way, the object queries could attend to the global image feature and capture the essential information for each predicted objects. In this section, we aim to explore how to build an attention-like mechanism with ConvNets while maintaining the capability similar to attention.

Self-interaction module (SIM). Take DETR as an example, given N object queries $o \in \mathbb{R}^{N \times d}$, we first reshape the queries to $\mathbb{R}^{w_q \times h_q \times d}$ and feed them into convolutional layers. For example, if we have $N = 100$ object queries, the query embeddings are reshaped into $\mathbb{R}^{10 \times 10 \times d}$. More design choices of reshaping will be discussed in ablation studies. As shown in Fig. 2 (b), the SIM part for DECO decoder is quite similar to the design scheme of DECO encoder, where stacking the depthwise convolution and 1×1 convolution could lead to strong capability similar to the self-attention mechanism. We utilize a large kernel convolution up to 9×9 to perform long-range perceptual feature extraction.

Cross-interaction module (CIM). The CIM mainly takes two features as input, *e.g.*, the image feature embeddings from the output of encoder ($z_e \in \mathbb{R}^{d \times H \times W}$), and the object query embeddings produced from the SIM part ($o \in \mathbb{R}^{w_q \times h_q \times d}$). The cross-attention mechanism in DETR decoder allows each object query to interact with the image features to capture necessary information for object prediction. However, using ConvNets to perform such kind of interaction is not so intuitive.

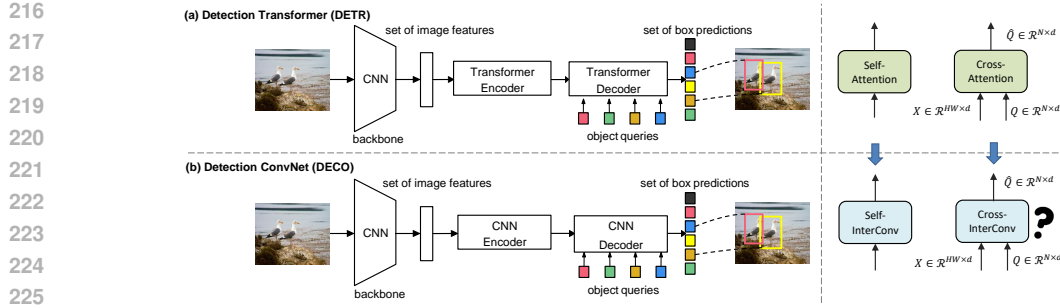


Figure 3: The overall architecture of DETR (Carion et al., 2020) and our proposed **Detection ConvNet (DECO)**. Our DECO is a simple yet effective query-based end-to-end object detection framework and enjoys the similar favorable attributes as DETR. Moreover, it is stacked with only standard convolutional layers and does not rely on any sophisticated attention modules.

As shown in Fig. 2 (b), we first upsample the object queries o to obtain $\hat{o} \in \mathbb{R}^{d \times H \times W}$ so that it has the same size with image feature z_e , i.e.,

$$\hat{o} = \text{Upsample}(o). \quad (1)$$

There are also other design choices for the upsampling function, i.e., resizing both the object queries and encoder embeddings to a fixed size before fusion, or directly upsampling the object queries to dynamic size of encoder embeddings, which is related to the resolution of input image. We will provide more analysis in experimental section. Then the upsampled object queries and the image feature embeddings are fused together using $\text{Fusion}(\cdot)$ function, followed by a large kernel depthwise convolution (Liu et al., 2023b; Ding et al., 2022; 2024) to allow object queries to capture the spatial information from the image feature. An intuitive implementation for $\text{Fusion}(\cdot)$ is element-wise *add* operation. There are also some alternatives like element-wise *multiply* operation, or first concatenating two features then using convolution to reduce the number of channels. More discussions will be presented in the ablation studies. The skip connection is all utilized, as shown in the following equation:

$$\hat{o}_f = \hat{o} + \text{dwconv}(\text{Fusion}(\hat{o}, z_e)). \quad (2)$$

The output features further go through another FFN with skip connection. Finally, an adaptive *maxpooling* is utilized to downsample the object queries back to the size of $\mathbb{R}^{w_q \times h_q \times d}$ and will be further processed by the following decoder layers.

$$\hat{o}_p = \text{Pooling}(\hat{o}_f + \text{FFN}(\hat{o}_f)). \quad (3)$$

The final output embeddings of the decoder will be fed into the detection head to obtain the class and bounding box prediction, which is similar to the original DETR.

3.2 DECO: DETECTION CONVNETS EQUIPPED WITH INTERCONV

Carion et al. (Carion et al., 2020) proposes the Detection Transformer (DETR) that models object detection as a set prediction problem and directly produces a fixed set of objects. As shown in Fig. 3 (a), DETR first utilizes a backbone to extract image features, and feeds them into a transformer encoder and decoder architecture. A fixed small set of learned object queries interact with the global image context to directly output the final set of object predictions. DETR streamlines the end-to-end object detection pipeline and has attracted great research interest due to the good accuracy and run-time performance (Zhu et al., 2021; Zhang et al., 2022; Dai et al., 2021b;a) for object detection. Although transformers have shown great power in computer vision tasks like image classification, object detection, segmentation etc., there are also some recent work that reveal the potential of ConvNet-based architecture as the common backbone, e.g., ConvNext (Liu et al., 2022b) and ConvFormer (Yu et al., 2022). In this work we re-examine the DETR design and explore whether a ConvNet-based object detector could inherit the good properties of DETR.

One of the most important properties for DETR-based detectors is the query-based scheme for producing the final predictions. In this way, the object detector could directly obtain a fixed number of objects and gets rid of any hand-designed NMS post-processing. We follow this paradigm to design our Detection ConvNets (DECO), as shown in Fig. 3 (b). DECO also utilizes a CNN backbone

270 Table 1: Comparisons of our proposed DECO+ with other detectors on COCO 2017 val set. The
 271 FPS is measured on a V100 GPU.

Model	Backbone	GFLOPs	FPS	AP	AP ₅₀	AP ₇₅	AP _S	AP _M	AP _L
Faster R-CNN (Ren et al., 2015)	R50-FPN	180	26	40.2	61.0	43.8	24.2	43.5	52.0
Faster R-CNN (Ren et al., 2015)	R101-FPN	246	20	42.0	62.5	45.9	25.2	45.6	54.6
FCOS (Tian et al., 2019)	R50-FPN	201	23	38.7	57.4	41.8	22.9	42.5	50.1
FCOS (Tian et al., 2019)	R101-FPN	277	19	39.1	58.3	42.1	22.7	43.3	50.3
RetinaNet (Lin et al., 2017)	R50-FPN	239	21	37.4	56.7	39.6	20.0	40.7	49.7
RetinaNet (Lin et al., 2017)	R101-FPN	315	17	38.5	57.6	41.0	21.7	42.8	50.4
Sparse R-CNN (Sun et al., 2021b)	R50-FPN	150	23	42.8	61.2	45.7	26.7	44.6	57.6
OneNet-RetinaNet (Sun et al., 2021a)	R50-FPN	239	21	37.5	55.4	40.7	21.5	40.5	47.4
OneNet-FCOS (Sun et al., 2021a)	R50-FPN	206	26	38.9	57.2	42.2	23.9	41.8	49.4
DeFCN (Wang et al., 2021a)	R50-FPN	—	19	41.4	59.5	45.6	26.1	44.9	52.0
YOLOS-Ti (Fang et al., 2021)	DeiT-Tiny	21	52	28.7	47.2	28.9	9.7	29.2	46.0
YOLOS-S (Fang et al., 2021)	DeiT-Small	194	5	36.1	55.7	37.6	15.6	38.3	55.3
YOLOS-B (Fang et al., 2021)	DeiT-Base	538	2	42.0	62.2	44.4	19.5	45.3	62.1
DETR (Carion et al., 2020)	R50	97	28	39.5	60.3	41.4	17.5	43.0	59.1
Deformable-DETR (Zhu et al., 2021)	R50	173	16	43.8	62.6	47.7	26.4	47.1	58.0
Anchor-DETR (Wang et al., 2022)	R50	103	21	42.1	63.1	44.9	22.3	46.2	60.0
DAB-DETR (Liu et al., 2022a)	R50	94	25	42.2	63.1	44.7	21.5	45.7	60.3
DN-DAB-DETR (Li et al., 2022)	R50	94	25	44.1	64.4	46.7	22.9	48.0	63.4
Cond-DETR (Meng et al., 2021)	R50	90	28	43.0	64.0	45.7	22.7	46.7	61.5
ViDT (Song et al., 2021)	Swin-Nano	35	31	40.4	59.6	43.3	23.2	42.5	55.8
DINO-4scale (Zhang et al., 2022)	R50	279	12	50.9	69.0	55.3	34.6	54.1	64.6
Stable-DINO (Liu et al., 2023a)	R50	—	12	51.5	68.5	56.3	35.2	54.7	66.5
SpeedDETR (Dong et al., 2023)	R50	—	21	46.8	66.2	50.4	28.5	50.6	63.2
DDQ-DETR (Zhang et al., 2023)	R50	—	9	52.8	69.9	58.1	37.4	55.7	66.0
Lite-DINO (Li et al., 2023)	R50	151	17	50.2	-	54.6	33.5	53.6	65.5
Co-DETR (Zong et al., 2022)	R50	-	12	49.5	67.6	54.3	32.4	52.7	63.7
H-DETR (Jia et al., 2022)	R50	280	19	50.0	68.3	54.4	32.9	52.7	65.3
Focus-DETR (Zheng et al., 2023)	R50	154	20	50.4	68.5	55.0	34.0	53.5	64.4
Rank-DETR (Pu et al., 2023)	R50	280	19	51.2	68.9	56.2	34.5	54.9	64.9
RT-DETR [†] (Lv et al., 2023)	R18	40	60	41.7	61.3	45.3	25.0	44.0	56.8
DECO+ (Ours)	R18	32	66	40.5	58.7	44.0	23.3	43.8	55.7
DECO+ (Ours)	R50	69	34	47.8	67.1	52.4	30.6	51.9	64.2
DECO+ (Ours)	ConvNeXt-B	159	20	50.6	70.7	55.0	34.4	55.3	67.8

303 to extract features from the input image. Specifically, given a RGB image $x_{\text{img}} \in \mathbb{R}^{3 \times H_0 \times W_0}$, the
 304 backbone generates feature map $f \in \mathbb{R}^{C \times H \times W}$ and usually $H, W = \frac{H_0}{32}, \frac{W_0}{32}$. The feature map f
 305 are then go through a CNN encoder to obtain the output embeddings $f_{\text{enc}} \in \mathbb{R}^{C_e \times H \times W}$. The CNN
 306 decoder takes f_{enc} as well as a fixed number of learned object queries $o \in \mathbb{R}^{N \times d}$ as input to make
 307 final detection prediction via a feed forward network (FFN), where d is the size of encoder output
 308 embeddings. The detailed architectures of the decoder are elaborated in the above section. We utilize
 309 the same prediction loss as in DETR, which uses bipartite matching to find paired predicted and
 310 ground truth objects.

311 **DECO Encoder.** Similar to DETR, a 1×1 convolution is first utilized to reduce the channel
 312 dimension of f from C to d and obtain a new feature map $z_0 \in \mathbb{R}^{d \times H \times W}$. In DETR, z_0 is fed
 313 into stacked transformer encoder layers, which mainly consists of multi-head self-attention (MHSA)
 314 and feed-forward network (FFN) to perform spatial and channel information mixing respectively.
 315 Recent work such as ConvNeXt (Liu et al., 2022b) has demonstrated that using stacked depthwise and
 316 pointwise convolutions could achieve comparable performance with Transformers. Therefore, we use
 317 the ConvNeXt blocks to build our DECO encoder. Specifically, each DECO encoder layer is stacked
 318 with a 7×7 depthwise convolution, a LayerNorm layer, a 1×1 convolution, a GELU activation and
 319 another 1×1 convolution. Besides, in DETR, positional encodings are necessary to be added to the
 320 input of each transformer encoder layer, since the transformer architecture is permutation-invariant.
 321 However, the ConvNet architecture is permutation-variant so that our DECO encoder layers could get
 322 rid of any positional encodings.

323 **DECO+ Equipped with Multi-scale Feature.** One limitation of original DETR as well as our DECO
 324 is the lack of multi-scale feature, which is demonstrated to be important for accurate object detection.

324 Table 2: Comparisons of DECO with DETR on COCO 2017. The FPS is measured on a V100 GPU.
325

Model	Backbone	GFLOPs	FPS	AP	AP ₅₀	AP ₇₅	AP _S	AP _M	AP _L
DETR (Carion et al., 2020)	R34	88	34	31.6	47.6	33.3	13.3	34.1	49.1
DETR (Carion et al., 2020)	R50	97	28	39.5	60.3	41.4	17.5	43.0	59.1
DETR (Carion et al., 2020)	ConvNeXt-T	104	25	42.1	63.6	44.3	18.8	45.5	62.8
DECO (Ours)	R50	103	35	38.6	58.8	41.1	19.5	43.3	55.0
DECO (Ours)	ConvNeXt-T	110	28	40.8	61.5	43.5	20.5	45.7	58.4

326 Deformable DETR (Zhu et al., 2021) utilizes the multi-scale deformable attention module to aggregate
 327 multi-scale features, but this mechanism can not be directly applied to our DECO framework. To
 328 equip DECO with multi-scale feature capability, we utilize the cross-scale feature-fusion module
 329 in RT-DETR (Lv et al., 2023) after obtaining the global feature from our DECO encoder. The
 330 features are then mapped to the same scale and concatenated along the channels followed by a linear
 331 projection layer to get the final encoder embeddings. More modern techniques for DETRs would also
 332 be compatible with DECO, which we leave for future exploration.

333 3.3 DECO-TINY SAM: INTERCONV FOR SEGMENT ANYTHING MODEL

341 The mechanism of InterConv could have great potential for applying to other architectures and tasks,
 342 especially for those involving interaction across domains. As a proof of concept, we replace the mask
 343 decoder in Segment Anything Model (SAM) with our DECO decoder. The motivation is that as a
 344 prompt-based segmentation model, SAM interacts between prompt tokens and image embeddings
 345 through the mask decoder which consists of self- and cross-attentions, sharing similar spirits of
 346 our proposed SIM and CIM. More specifically, we repeat the one-dimensional queries into two
 347 dimensional features, instead of reshaping queries as in object detection task discussed above. It
 348 is mainly due to the fact that the query tokens in SAM contains learnable output tokens and a few
 349 prompt tokens, which are not reasonable to simply be reshaped into two dimensions. We utilize
 350 TinySAM (Shu et al., 2023) as the baseline model and replace the decoder to our proposed DECO
 351 architecture.

352 4 EXPERIMENTS

353 In this section, we first evaluate our proposed model on object detection benchmark and compare
 354 it against state-of-the-art methods. Extensive ablation studies are also conducted to provide more
 355 discussions and insights about the design choices.

356 4.1 EXPERIMENTAL SETTING

357 **Dataset.** All experiments are conducted on the challenging COCO 2017 (Lin et al., 2014) detection
 358 benchmark, which contains about 118K training images and 5K validation samples.

359 **Training.** For the vanilla DECO, we follow similar training settings as DETR (Carion et al., 2020).
 360 We train the proposed DECO models for 150 epochs using AdamW optimizer, with weight decay of
 361 10^{-4} and initial learning rates as 10^{-4} and 10^{-5} for the encoder-decoder and backbone, respectively.
 362 The learning rate is dropped by a factor of 10 after 100 epochs. The augmentation scheme is the
 363 same as DETR, which includes random horizontal flipping, random crop augmentation, and scale
 364 augmentation. The input image shorter side is resized to a random size between 480 and 800 pixels in
 365 the scale augmentation while restricting the longer size to at most 1333. As to DECO+ that equipped
 366 with multi-scale feature fusion, the training image size is selected between 480 and 800 with 32 stride
 367 following the RT-DETR baseline. The inference size is set to 640×640 .

368 4.2 COMPARISONS WITH STATE-OF-THE-ARTS

369 We evaluate the proposed DECO and DECO+ on COCO benchmark and compare with recent
 370 competitive object detectors, including DETR (Carion et al., 2020), YOLOS (Fang et al., 2021),
 371 FCOS (Tian et al., 2019), and DETR variants with strong performance, e.g., Anchor-DETR (Sun et al.,
 372 2021b), Conditional-DETR (Sun et al., 2021a) and ViDT. (Wang et al., 2021a) etc.. Experimental
 373 results in terms of detection AP and FLOPs/FPS are shown in Table 1. The FPS we report is the

Fusion Method	GFLOPS	AP
Element-wise Mult.	103	37.8
Concat-Conv	106	38.6
Element-wise Add	103	38.6

383 Table 3: Effect of different fusion methods.

384 Table 5: Ablation studies for different kernel sizes in decoder.

385 Table 4: Effect of number of layers in decoder.

kernel size	5×5	7×7	9×9	11×11	13×13	15×15
AP (%)	37.8	37.9	38.6	38.6	38.4	38.6
GFLOPs	103.35	103.47	103.58	103.70	104.11	104.27

389 average number of the first 100 images in the COCO 2017 *val* set on a NVIDIA V100 GPU. The
390 FLOPs are computed with the input size of (640, 640) for RT-DETR and the proposed DECO+, while
391 (1280, 800) for others. A more intuitive comparison of the trade-off between AP and latency is also
392 shown in Fig. 1.

393 **Comparisons with DETR variants.** We consider different ConvNet-based backbones for DECO+
394 in the benchmarking. As shown in Table 1, our DECO+ with ResNet-50 Backbone achieves 47.8%
395 AP with 34 FPS on V100 GPU, which is better than most previous DETR variants considering the
396 accuracy-latency trade-off. The ConvNeXt (Liu et al., 2022b) based DECO+ achieves an even higher
397 AP at 50.6% which is 0.2% higher than Focus-DETR (Zheng et al., 2023) at the same FPS. Moreover,
398 ResNet-18 based DECO+ obtains 40.5% AP with 66 FPS, achieving quite similar performance with a
399 variant of RT-DETR (Lv et al., 2023) that we modified to not use deformable attention and denoising
400 training for fair comparison. Note that deformable attention and denoising training is specifically
401 designed for attention-based architecture, and similar improved strategies for DECO still remains for
402 future exploration.

403 **Comparisons with Other End-to-End Detectors.** YOLOS is an encoder-only Transformer archi-
404 tecture for object detection based on the vanilla pre-trained vision transformers. Our DECO+ models
405 show clear advantage over YOLOS and have similar detection performance while running much
406 faster. We also compare our DECO+ with recent end-to-end detectors with ConvNets, *e.g.*, Sparse
407 R-CNN (Sun et al., 2021b), OneNet (Sun et al., 2021a) and DeFCN. (Wang et al., 2021a). As shown
408 in Table 1, our DECO+ outperforms Sparse R-CNN (Sun et al., 2021b) and OneNet-RetinaNet (Sun
409 et al., 2021a) with better accuracy and running speed. Similarly, DECO+ obtains 47.8% AP and 34
410 FPS while DeFCN (Wang et al., 2021a) only has 19 FPS with 41.4% AP.

411 **Comparisons with DETR.** We compare the performance of our vanilla DECO and DETR (Car-
412 ion et al., 2020) equipped with ResNet and ConvNeXt-Tiny in Table 2. The proposed DECO
413 encoder/decoder are adopted to substitute the transformer encoder/decoder in DETR for comparison.
414 To align the FLOPs with DETR, we modify the DECO encoder to be three stages with the number of
415 blocks of (2, 6, 2) and the channel dimension of (120, 240, 480), respectively. As shown in Table 2,
416 for both ResNet-50 and ConvNeXt-Tiny (Liu et al., 2022b) backbones, despite higher FLOPs, our
417 DECO obtain faster inference speed (FPS) than DETR. It demonstrates that our pure ConvNet-based
418 architecture is more deployment-friendly than the transformer-based DETR in GPU platform. Specif-
419 ically, our DECO obtains 38.6% AP at 35 FPS and is 7.0% AP better than DETR with ResNet-34
420 backbone for similar running speed.

421 4.3 ABLATION STUDIES

423 We conduct extensive ablation studies based on the R50-based DECO in Table 2 to provide more
424 discussions and insights about different design choices and justify the effectiveness of our proposed
425 method.

426 **Upsampling Size in CIM.** In CIM, the object queries are first upsampled and then fused with the
427 encoder embeddings to deal with different dimensions. Here we have different design choices, *i.e.*,
428 resizing both the object queries and encoder embeddings to a fixed size before fusion, or directly
429 upsampling the object queries to dynamic size of encoder embeddings, which is related to the
430 resolution of input image. As shown in Table 6, utilizing dynamic size achieves the best performance,
431 since it is more flexible for different input resolution and has no information discarding. Noted that
(25 × 38) is the average size of COCO training set and it leads to 0.5 AP drop than dynamic way.

	Size	GFLOPs	AP
432	(20 × 20)	97	34.8
433	(25 × 38)	103	38.1
434	(40 × 40)	110	37.2
435	Dynamic	103	38.6
436			
437			

Table 6: Effect of different upsampling size of object queries in CIM.

#queries	Query Shape ($w_q \times h_q$)	Ratio	AP
100	10 × 10	1:1	38.6
100	20 × 5	4:1	38.3
100	5 × 20	1:4	36.9
300	30 × 10	3:1	38.9
300	20 × 15	4:3	38.8

Table 7: Effect of different shape of queries.

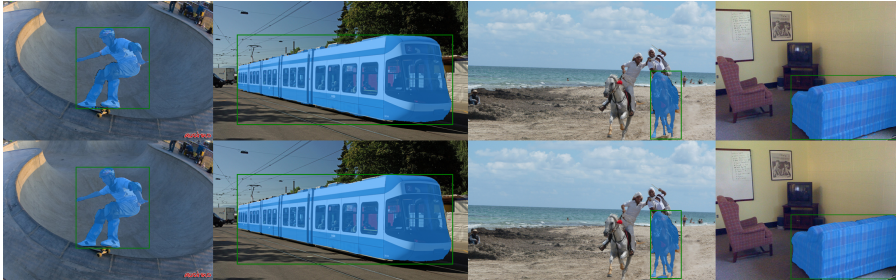


Figure 4: Visualizations for box prompted segment anything for Our DECO-TinySAM (1st row) and TinySAM (2nd row). Our method obtains quite similar performance with TinySAM.

Number of Decoder Layers. As shown in Table 4, more number of layers in decoder tends to have better performance. However, utilizing 6 decoder layers is a good choice to balance performance and computational cost and we keep this choice following DETR (Carion et al., 2020).

Kernel size in decoder. The motivation for using 9×9 dwconv is to enable sufficient receptive field. We conduct ablation experiments to explore the effect of different kernel sizes. As shown in Table 5, using 5×5 has unsatisfied performance due to limited receptive field, and enlarging kernel size to 11×11 or even 15×15 brings negligible improvement.

Different design choices of fusion method in CIM. As discussed in Section 3, the upsampled object queries and the image feature embeddings are fused together using *add* operations. Here we conduct ablation studies for other design choices of the fusion method, *e.g.*, using concatenation and convolution, or simple conducting element-wise multiplication for fusion. As shown in Table 3, utilizing element-wise multiplication to fuse the object queries and the image feature embeddings does not obtain better performance. Moreover, using *add* operations achieves similar detection performance with using concatenation and convolution, but has slightly smaller FLOPs.

Different shapes of object queries. In our proposed method, the object queries should be in 2D shape of $w_q \times h_q$ and there are several choices of query shape for N object queries. For example, $w_q \times h_q$ could be 10×10 , 20×5 or 5×20 for $N = 100$ queries. As shown in Table 7, using 10×10 obtains better detection performance. When $N = 300$, using query shape of 30×10 achieves slightly better performance than 20×15 . A typical ratio of image size for COCO could be considered as $1333 : 800 \approx 1.67$ and we could conclude from Table 7 that better performance is obtained when the query shape is approximately the ratio of input image.

4.4 EXTENSION TO SEGMENT ANYTHING TASK

Our proposed DECO is original designed for object detection. However, the mechanism of DECO decoder could have great potential for applying to other architectures and tasks, especially for those involving interaction across domains. As a proof of concept, we replace the mask decoder in

Method	COCO AP (%)	Mobile Lat. (ms)
TinySAM (Shu et al., 2023)	41.9	34
DECO-TinySAM	41.4	29

Table 8: Zero-shot instance segmentation results for TinySAM baseline and our DECO-TinySAM.

Segment Anything Model (SAM) with our DECO decoder. The motivation is that as a prompt-based segmentation model, SAM interacts between prompt tokens and image embeddings through the mask decoder which consists of self- and cross-attentions, sharing similar spirits of our proposed SIM and CIM. More specifically, we repeat the one-dimensional queries into two dimensional features, instead

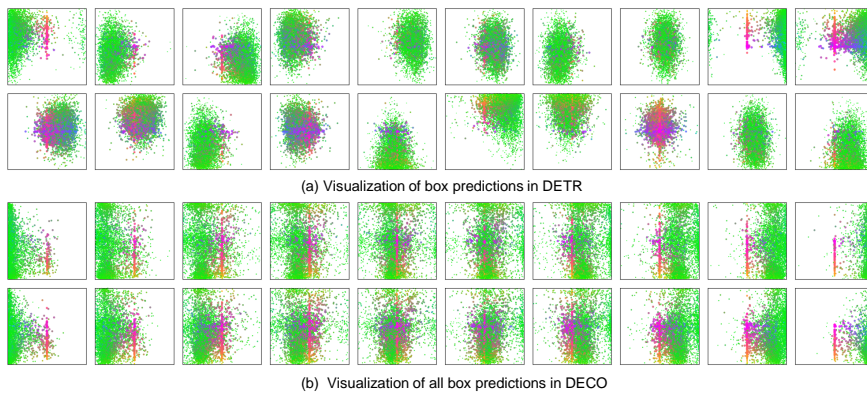


Figure 5: Visualizations of query slots for DETR and our DECO. We can find that both DECO and DETR tend to make different object queries to focus on different patterns in terms of spatial areas and box sizes. Interestingly, we could also observe that the slots of DETR for small objects are spatially unordered while the distributions of each slot for our DECO are spatially ordered for small boxes.

of reshaping queries as in object detection task discussed above. It is mainly due to the fact that the query tokens in SAM contains learnable output tokens and a few prompt tokens, which are not reasonable to simply be reshaped into two dimensions.

We utilize TinySAM (Shu et al., 2023) as the baseline model and replace the decoder to our proposed InterConv architecture. The results for zero-shot instance segmentation prompted by detected boxes on COCO dataset are shown in Table 8. Despite without carefully tuning, our DECO-TinySAM obtains quite similar zero-shot instance segmentation performance with that of TinySAM baseline, with lower latency on mobile devices. We also provide some visualizations for box prompted segment anything for our DECO-TinySAM and the TinySAM baseline, demonstrating strong performance and generalizability to other tasks of our method.

4.5 VISUALIZATION

Visualization of Query Slots. Following the same method in DETR, we visualize the boxes predicted by 20 out of total 100 query slots of our DECO. Each point represents one bounding box prediction and the coordinates are normalized by each image size. Different colors indicate objects with different scales, e.g., green, red and blue refer to small boxes, large horizontal boxes and large vertical boxes, respectively. As shown in Fig. 5, we can find that both DECO and DETR tend to make different object queries to focus on different patterns in terms of spatial areas and box sizes. Interestingly, we could also observe that the slots of DETR for small objects are spatially unordered, which indicates that the prediction of each slot is random in spatial dimension. However, things are a bit different for our DECO, whose distributions of each slot are spatially ordered for small boxes. This observation is most likely to be related to the cross-interaction mechanism of object queries and image features, where cross-attention module tends to capture global information and our proposed module tends to focus on local interaction through large kernel convolutions.

5 CONCLUSION AND DISCUSSION

In this paper, we aim to explore whether we could build query-based detection and segmentation framework with ConvNets instead of sophisticated transformer architecture. We propose a novel mechanism dubbed InterConv to perform interaction between object queries and image features via convolutional layers. Equipped with the proposed InterConv, we build Detection ConvNet (DECO), which is composed of a backbone and convolutional encoder-decoder architecture. We compare the proposed DECO against prior detectors on the challenging COCO benchmark. Despite its simplicity, our DECO achieves competitive performance in terms of detection accuracy and running speed. Specifically, with the ResNet-18 and ResNet-50 backbone, our DECO achieves 40.5% and 47.8% AP with 66 and 34 FPS, respectively. The proposed method is also evaluated on the segment anything task, demonstrating similar performance and higher efficiency. We hope the proposed method brings another perspective for designing architectures for vision tasks.

540 REFERENCES
541

- 542 Alexey Bochkovskiy, Chien-Yao Wang, and Hong-Yuan Mark Liao. Yolov4: Optimal speed and
543 accuracy of object detection. *CoRR*, abs/2004.10934, 2020.
- 544 Zhaowei Cai and Nuno Vasconcelos. Cascade r-cnn: Delving into high quality object detection. In
545 *CVPR*, pp. 6154–6162, 2018.
- 546 Nicolas Carion, Francisco Massa, Gabriel Synnaeve, Nicolas Usunier, Alexander Kirillov, and Sergey
547 Zagoruyko. End-to-end object detection with transformers. In *ECCV*, pp. 213–229. Springer, 2020.
- 548 Tianheng Cheng, Xinggang Wang, Shaoyu Chen, Wenqiang Zhang, Qian Zhang, Chang Huang,
549 Zhaoxiang Zhang, and Wenyu Liu. Sparse instance activation for real-time instance segmentation.
550 In *Proceedings of the IEEE/CVF Conference on Computer Vision and Pattern Recognition*, pp.
551 4433–4442, 2022.
- 552 Xiyang Dai, Yinpeng Chen, Jianwei Yang, Pengchuan Zhang, Lu Yuan, and Lei Zhang. Dynamic
553 detr: End-to-end object detection with dynamic attention. In *ICCV*, pp. 2988–2997, 2021a.
- 554 Zhigang Dai, Bolun Cai, Yugeng Lin, and Junying Chen. Up-detr: Unsupervised pre-training for
555 object detection with transformers. In *CVPR*, pp. 1601–1610, 2021b.
- 556 Xiaohan Ding, Xiangyu Zhang, Jungong Han, and Guiguang Ding. Scaling up your kernels to 31x31:
557 Revisiting large kernel design in cnns. In *Proceedings of the IEEE/CVF conference on computer
558 vision and pattern recognition*, pp. 11963–11975, 2022.
- 559 Xiaohan Ding, Yiyuan Zhang, Yixiao Ge, Sijie Zhao, Lin Song, Xiangyu Yue, and Ying Shan.
560 Unireplknet: A universal perception large-kernel convnet for audio video point cloud time-series
561 and image recognition. In *Proceedings of the IEEE/CVF Conference on Computer Vision and
562 Pattern Recognition*, pp. 5513–5524, 2024.
- 563 Peiyan Dong, Zhenglun Kong, Xin Meng, Peng Zhang, Hao Tang, Yanzhi Wang, and Chih-Hsien
564 Chou. Speeddetr: Speed-aware transformers for end-to-end object detection. In *International
565 Conference on Machine Learning*, pp. 8227–8243. PMLR, 2023.
- 566 Alexey Dosovitskiy, Lucas Beyer, Alexander Kolesnikov, Dirk Weissenborn, Xiaohua Zhai, Thomas
567 Unterthiner, Mostafa Dehghani, Matthias Minderer, Georg Heigold, Sylvain Gelly, et al. An image
568 is worth 16x16 words: Transformers for image recognition at scale. In *ICLR*, 2021.
- 569 Kaiwen Duan, Song Bai, Lingxi Xie, Honggang Qi, Qingming Huang, and Qi Tian. Centernet:
570 Keypoint triplets for object detection. In *ICCV*, 2019.
- 571 Yuxin Fang, Bencheng Liao, Xinggang Wang, Jiemin Fang, Jiyang Qi, Rui Wu, Jianwei Niu, and
572 Wenyu Liu. You only look at one sequence: Rethinking transformer in vision through object
573 detection. *NeurIPS*, 34:26183–26197, 2021.
- 574 Peng Gao, Minghang Zheng, Xiaogang Wang, Jifeng Dai, and Hongsheng Li. Fast convergence of
575 detr with spatially modulated co-attention. In *ICCV*, pp. 3621–3630, 2021.
- 576 Shang-Hua Gao, Ming-Ming Cheng, Kai Zhao, Xin-Yu Zhang, Ming-Hsuan Yang, and Philip Torr.
577 Res2net: A new multi-scale backbone architecture. *IEEE transactions on pattern analysis and
578 machine intelligence*, 43(2):652–662, 2019.
- 579 Jianyuan Guo, Kai Han, Yunhe Wang, Chao Zhang, Zhaohui Yang, Han Wu, Xinghao Chen, and
580 Chang Xu. Hit-detector: Hierarchical trinity architecture search for object detection. In *CVPR*, pp.
581 11405–11414, 2020.
- 582 Kaiming He, Xiangyu Zhang, Shaoqing Ren, and Jian Sun. Deep residual learning for image
583 recognition. In *CVPR*, pp. 770–778, 2016.
- 584 Ding Jia, Yuhui Yuan, Haodi He, Xiaopei Wu, Haojun Yu, Weihong Lin, Lei Sun, Chao Zhang, and
585 Han Hu. Detrs with hybrid matching. *arXiv preprint arXiv:2207.13080*, 2022.
- 586 Tao Kong, Fuchun Sun, Huaping Liu, Yuning Jiang, and Jianbo Shi. Foveabox: Beyond anchor-based
587 object detector. *CoRR*, abs/1904.03797, 2019.

- 594 Hei Law, Yun Teng, Olga Russakovsky, and Jia Deng. Cornernet-lite: Efficient keypoint based object
 595 detection. In *BMVC*. BMVA Press, 2020. URL <https://www.bmvc2020-conference.com/assets/papers/0016.pdf>.
- 596
- 597 Feng Li, Hao Zhang, Shilong Liu, Jian Guo, Lionel M Ni, and Lei Zhang. Dn-detr: Accelerate detr
 598 training by introducing query denoising. *arXiv preprint arXiv:2203.01305*, 2022.
- 599
- 600 Feng Li, Ailing Zeng, Shilong Liu, Hao Zhang, Hongyang Li, Lei Zhang, and Lionel M Ni. Lite detr:
 601 An interleaved multi-scale encoder for efficient detr. *arXiv preprint arXiv:2303.07335*, 2023.
- 602
- 603 Yanghao Li, Yuntao Chen, Naiyan Wang, and Zhaoxiang Zhang. Scale-aware trident networks for
 604 object detection. In *ICCV*, pp. 6054–6063, 2019.
- 605
- 606 Zeming Li, Chao Peng, Gang Yu, Xiangyu Zhang, Yangdong Deng, and Jian Sun. Detnet: Design
 607 backbone for object detection. In *ECCV*, pp. 334–350, 2018.
- 608
- 609 Tsung-Yi Lin, Michael Maire, Serge Belongie, James Hays, Pietro Perona, Deva Ramanan, Piotr
 610 Dollár, and C Lawrence Zitnick. Microsoft coco: Common objects in context. In *ECCV*, pp.
 740–755, 2014.
- 611
- 612 Tsung-Yi Lin, Priya Goyal, Ross Girshick, Kaiming He, and Piotr Dollár. Focal loss for dense object
 613 detection. In *ICCV*, pp. 2980–2988, 2017.
- 614
- 615 Shilong Liu, Feng Li, Hao Zhang, Xiao Yang, Xianbiao Qi, Hang Su, Jun Zhu, and Lei Zhang.
 616 Dab-detr: Dynamic anchor boxes are better queries for detr. In *ICLR*, 2022a.
- 617
- 618 Shilong Liu, Tianhe Ren, Jiayu Chen, Zhaoyang Zeng, Hao Zhang, Feng Li, Hongyang Li, Jun
 619 Huang, Hang Su, Jun Zhu, et al. Detection transformer with stable matching. In *Proceedings of
 the IEEE/CVF International Conference on Computer Vision*, pp. 6491–6500, 2023a.
- 620
- 621 Shiwei Liu, Tianlong Chen, Xiaohan Chen, Xuxi Chen, Qiao Xiao, Boqian Wu, Tommi Kärkkäinen,
 622 Mykola Pechenizkiy, Decebal C Mocanu, and Zhangyang Wang. More convnets in the 2020s:
 623 Scaling up kernels beyond 51x51 using sparsity. In *International Conference on Learning Representations, ICLR 2023*, 2023b.
- 624
- 625 Wei Liu, Dragomir Anguelov, Dumitru Erhan, Christian Szegedy, Scott E. Reed, Cheng-Yang Fu,
 626 and Alexander C. Berg. SSD: single shot multibox detector. In *ECCV*, 2016.
- 627
- 628 Yudong Liu, Yongtao Wang, Siwei Wang, TingTing Liang, Qijie Zhao, Zhi Tang, and Haibin Ling.
 629 Cbnet: A novel composite backbone network architecture for object detection. In *AAAI*, volume 34,
 pp. 11653–11660, 2020.
- 630
- 631 Ze Liu, Yutong Lin, Yue Cao, Han Hu, Yixuan Wei, Zheng Zhang, Stephen Lin, and Baining
 632 Guo. Swin transformer: Hierarchical vision transformer using shifted windows. In *ICCV*, pp.
 10012–10022, 2021.
- 633
- 634 Zhuang Liu, Hanzi Mao, Chao-Yuan Wu, Christoph Feichtenhofer, Trevor Darrell, and Saining Xie.
 635 A convnet for the 2020s. In *CVPR*, pp. 11976–11986, 2022b.
- 636
- 637 Xin Lu, Buyu Li, Yuxin Yue, Quanquan Li, and Junjie Yan. Grid R-CNN. In *CVPR*, 2019.
- 638
- 639 Wenyu Lv, Shangliang Xu, Yian Zhao, Guanzhong Wang, Jinman Wei, Cheng Cui, Yuning Du,
 640 Qingqing Dang, and Yi Liu. Detrs beat yolos on real-time object detection. *arXiv preprint
 arXiv:2304.08069*, 2023.
- 641
- 642 Depu Meng, Xiaokang Chen, Zejia Fan, Gang Zeng, Houqiang Li, Yuhui Yuan, Lei Sun, and Jingdong
 643 Wang. Conditional detr for fast training convergence. In *ICCV*, 2021.
- 644
- 645 Alexander Neubeck and Luc Van Gool. Efficient non-maximum suppression. In *ICPR*, volume 3, pp.
 850–855, 2006.
- 646
- 647 Jiangmiao Pang, Kai Chen, Jianping Shi, Huajun Feng, Wanli Ouyang, and Dahua Lin. Libra R-CNN:
 648 towards balanced learning for object detection. In *CVPR*, 2019.

- 648 Yifan Pu, Weicong Liang, Yiduo Hao, Yuhui Yuan, Yukang Yang, Chao Zhang, Han Hu, and Gao
 649 Huang. Rank-detr for high quality object detection. In *NeurIPS*, 2023.
 650
- 651 Joseph Redmon and Ali Farhadi. YOLO9000: better, faster, stronger. In *CVPR*, 2017.
 652
- 653 Joseph Redmon and Ali Farhadi. Yolov3: An incremental improvement. *CoRR*, abs/1804.02767,
 654 2018.
- 655 Joseph Redmon, Santosh Kumar Divvala, Ross B. Girshick, and Ali Farhadi. You only look once:
 656 Unified, real-time object detection. In *CVPR*, 2016.
 657
- 658 Shaoqing Ren, Kaiming He, Ross Girshick, and Jian Sun. Faster R-CNN: Towards real-time object
 659 detection with region proposal networks. *NeurIPS*, 28, 2015.
 660
- 661 Han Shu, Wenshuo Li, Yehui Tang, Yiman Zhang, Yihao Chen, Houqiang Li, Yunhe Wang, and
 662 Xinghao Chen. Tinysam: Pushing the envelope for efficient segment anything model. *arXiv
 preprint arXiv:2312.13789*, 2023.
 663
- 664 Hwanjun Song, Deqing Sun, Sanghyuk Chun, Varun Jampani, Dongyoon Han, Byeongho Heo,
 665 Wonjae Kim, and Ming-Hsuan Yang. Vidt: An efficient and effective fully transformer-based
 666 object detector. In *ICLR*, 2021.
- 667 Peize Sun, Yi Jiang, Enze Xie, Wenqi Shao, Zehuan Yuan, Changhu Wang, and Ping Luo. What
 668 makes for end-to-end object detection? In *ICML*, pp. 9934–9944. PMLR, 2021a.
 669
- 670 Peize Sun, Rufeng Zhang, Yi Jiang, Tao Kong, Chenfeng Xu, Wei Zhan, Masayoshi Tomizuka, Lei
 671 Li, Zehuan Yuan, Changhu Wang, et al. Sparse r-cnn: End-to-end object detection with learnable
 672 proposals. In *CVPR*, pp. 14454–14463, 2021b.
 673
- 674 Zhi Tian, Chunhua Shen, Hao Chen, and Tong He. Fcos: Fully convolutional one-stage object
 675 detection. In *ICCV*, pp. 9627–9636, 2019.
 676
- 677 Hugo Touvron, Matthieu Cord, Matthijs Douze, Francisco Massa, Alexandre Sablayrolles, and Hervé
 678 Jégou. Training data-efficient image transformers & distillation through attention. In *ICML*, pp.
 10347–10357. PMLR, 2021.
 679
- 680 Fengbin Tu, Zihan Wu, Yiqi Wang, Ling Liang, Liu Liu, Yufei Ding, Leibo Liu, Shaojun Wei,
 681 Yuan Xie, and Shouyi Yin. Trancim: Full-digital bitline-transpose cim-based sparse transformer
 682 accelerator with pipeline/parallel reconfigurable modes. *IEEE Journal of Solid-State Circuits*,
 2022.
 683
- 684 Jianfeng Wang, Lin Song, Zeming Li, Hongbin Sun, Jian Sun, and Nanning Zheng. End-to-end
 685 object detection with fully convolutional network. In *CVPR*, pp. 15849–15858, 2021a.
 686
- 687 Wenhui Wang, Enze Xie, Xiang Li, Deng-Ping Fan, Kaitao Song, Ding Liang, Tong Lu, Ping Luo,
 688 and Ling Shao. Pyramid vision transformer: A versatile backbone for dense prediction without
 689 convolutions. In *ICCV*, pp. 568–578, 2021b.
 690
- 691 Yingming Wang, Xiangyu Zhang, Tong Yang, and Jian Sun. Anchor detr: Query design for
 692 transformer-based detector. In *AAAI*, volume 36, pp. 2567–2575, 2022.
 693
- 694 Weihao Yu, Chenyang Si, Pan Zhou, Mi Luo, Yichen Zhou, Jiashi Feng, Shuicheng Yan, and Xinchao
 695 Wang. Metaformer baselines for vision. *arXiv preprint arXiv:2210.13452*, 2022.
 696
- 697 Hao Zhang, Feng Li, Shilong Liu, Lei Zhang, Hang Su, Jun Zhu, Lionel Ni, and Harry Shum. Dino:
 698 Detr with improved denoising anchor boxes for end-to-end object detection. In *ICLR*, 2022.
 699
- 700 Shifeng Zhang, Cheng Chi, Yongqiang Yao, Zhen Lei, and Stan Z. Li. Bridging the gap between
 701 anchor-based and anchor-free detection via adaptive training sample selection. In *CVPR*, 2020.
 702
- 703 Shilong Zhang, Xinjiang Wang, Jiaqi Wang, Jiangmiao Pang, Chengqi Lyu, Wenwei Zhang, Ping
 704 Luo, and Kai Chen. Dense distinct query for end-to-end object detection. In *Proceedings of the
 705 IEEE/CVF conference on computer vision and pattern recognition*, pp. 7329–7338, 2023.
 706

- 702 Dehua Zheng, Wenhui Dong, Hailin Hu, Xinghao Chen, and Yunhe Wang. Less is more: Focus
703 attention for efficient detr, 2023.
- 704
- 705 Xingyi Zhou, Dequan Wang, and Philipp Krähenbühl. Objects as points. *CoRR*, abs/1904.07850,
706 2019. URL <http://arxiv.org/abs/1904.07850>.
- 707
- 708 Chenchen Zhu, Yihui He, and Marios Savvides. Feature selective anchor-free module for single-shot
709 object detection. In *CVPR*, 2019.
- 710
- 711 Chenchen Zhu, Fangyi Chen, Zhiqiang Shen, and Marios Savvides. Soft anchor-point object detection.
712 In *ECCV*, 2020. doi: 10.1007/978-3-030-58545-7_6. URL https://doi.org/10.1007/978-3-030-58545-7_6.
- 713
- 714 Xizhou Zhu, Weijie Su, Lewei Lu, Bin Li, Xiaogang Wang, and Jifeng Dai. Deformable detr:
715 Deformable transformers for end-to-end object detection. In *ICLR*, 2021.
- 716
- 717 Zhuofan Zong, Guanglu Song, and Yu Liu. Detrs with collaborative hybrid assignments training,
718 2022.
- 719
- 720
- 721
- 722
- 723
- 724
- 725
- 726
- 727
- 728
- 729
- 730
- 731
- 732
- 733
- 734
- 735
- 736
- 737
- 738
- 739
- 740
- 741
- 742
- 743
- 744
- 745
- 746
- 747
- 748
- 749
- 750
- 751
- 752
- 753
- 754
- 755